Indian J. Phys. **74B** (6), 455–462 (2000)

IJP B
international journal

Projectile charge signature of double ionisation—a QED approach

Sujata Bhattacharyya* and Kinkini Pathak
Gokhale Memorial Girls' College, Calcutta-700 020, India
E-mail : sbgcmr@cal2.vsnl.net.in

Received 13 October 1999, accepted 7 September 2000

Abstract A field theoretic calculation of the cross sections for the double ionization (DI) of H_2 by e$^-$, p$^+$ and fully stripped He^{2+}, Li^{3+} ions, is reported. In the medium high energy range, DI by electron is found to be greater than that by equivelocity proton. Dependence on projectile charge Z_p in the form of Z_p^3 is obtained in the ratios of DI cross sections between light stripped ions and proton. Present result is compared with available experimental results.

Keywords Double ionization cross section, field theoretic calculation, projectile charge signature

PACS Nos. : 34.10.+x, 34.50.Fa, 34.70.+e

1. Introduction

A good number of experiments have been done on double ionization of H_2 and D_2 [1–3] by fast fully stripped ions, electrons and protons. In those experiments, measurements of the ratio of the dissociative ionization cross section to non-dissociative ionization cross section in H_2 and D_2 were done, which served as a useful parameter in probing the electron correlation effects. Electronic correlation is also responsible for providing differences in the double ionization cross sections by positive and negative projectiles. In this paper, we present the study of the projectile charge signature on the cross sections for double ionization of H_2 in a QED approach. It was experimentally demonstrated that in the cases of two electron targets He and H_2 [4–8], the negative projectiles (e^-,p^-) have about twice the cross section for DI as do positive projectiles (e^+,p^+). Different theoretical models have been developed [9–13] to explain this difference. Reading and Ford [9] developed forced-impulse method to calculate DI of He.

Several different interaction mechanisms are known to produce DI [14a,b]. Present paper deals with the double ionization of H_2 by e^-, p^+, He^{2+}, Li^{3+}, in a field theoretic technique. This technique is successfully applied [15–19] to study charge transfer, ionization and excitation phenomena. Important Feynman diagrams contributing to DI are shown in Figure 1. These are shake-off (SO) process (Figure 1a), two-step-two (TS2) process (Figure 1b) and two-step-one (TS1) process (Figure 1c). Figure 1a gives rise to second order S-matrix (e^2 order in Born approximation). In SO

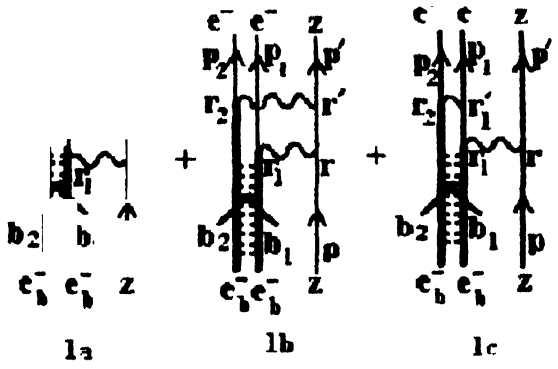

Figure 1. Feynman diagram for double ionization H_2 by projectiles of charge Z. The wavy lines represent virtual photon, straight arrowed lines represent electrons (e$^-$) and projectile of charge z. The bound electons are represented by thick lines and broken lines represent Coulomb photon exchange between the bound electrons. Figure 1a corresponds to shake-off process and Figures 1b and 1c correspond respectively to TS-2 and TS-1 processes.

mechanism, ejection of one of the bound electrons occurs due to current-current interaction between the projectile and the bound electron, while the other electron is emitted due to change in the Coulomb field of the nuclei. The correlated wave function takes care of the Coulomb effects. Eventually,

*Present Address : 370/1, N.S.C. Bose Road, Calcutta-700 047, India

Figure 1a can be identified with both the SO mechanism of McGuire [10] and the Goldstone diagram [14a] representing single collision and ground state correlation. Contribution from this term is proportional to the projectile charge Z_p. In the diagram 1b, the projectile exchanges two virtual photons, one each with two bound electrons. This gives rise to the fourth-order S-matrix (second order in Born approximation). Figure 1b can be identified with both the double collision mechanism (TS2) of McGuire and the double collision diagram of Goldstone. Contribution from this diagram is proportional to Z_p^2. In TS1 process (Figure 1c), virtual photon exchange between the projectile and one of the bound electrons causes ejection of that electron The resulting ionized electron in turn, exchanges a photon with the remaining bound electron and ejects it. Contribution from this diagram is proportional to Z_p. This two-step-one (TS1) mechanism can be identified with one of the Goldstone diagrams (Figure 1c of Ref. [14a]). Although we are considering second order and fourth order Feynman diagrams which are first and second order respectively in particle-radiation-field coupling, we can obtain results accurate to all orders in Coulomb coupling by a suitable choice of the wave function. The Sommerfeld-Maue relativistic wave function is well-suited for describing the incoming distorted wave projectile. To estimate the effect of this additional Coulomb coupling over the S-matrix particle-radiation-field coupling, we can multiply the cross section by the Sommerfeld factor [15]. However, we find that for energies above 100 keV/amu, it introduces negligible correction [18].

Recent studies [5,7] on DI of He by He^{2+} have shown that the TS2 process is mainly responsible near about 1000 keV/amu. At much higher velocities, the SO process dominates. At intermediate range of velocities, both the processes contribute. McGuirre has shown that the factor of two difference in DI by –ve and +ve projectiles is due to interference between TS2 and SO processes.

Experiment on double ionization of H_2 is done in a crossed beam technique [14a,b]. In high energy encounters, the dissociated fragments (H^+) move with equal and opposite momenta and the projectile moves forward with little loss of momentum. Eventually, energies of the ejected electrons are small. Under this situation, one may argue that contribution from the TS1 mechanism (Figure 1c) will be negligible, as it requires emission of energetic electron to initiate electron-electron interaction for ejection of the remaining bound electron.

We shall consider only the Feynman diagrams (Figure 1a and Figure 1b) for computing the double ionization of H_2 by +ve and –ve projectiles in the energy range of 1000 keV/amu to 4000 keV/amu as in the experiments [14a,b]. Contributions from the Figures 1a and 1b along with their interference term are computed separately in the following sections. The interference term is found to be proportional to Z_p^3 and decides the difference in the magnitude of DI by the projectiles of positive and negative charges.

2. Theory

The covariant interaction S_{SO} due to the second order Feynman diagram (Figure 1a) is given by the current-current interaction between the projectile and a bound electron of the two-electron target. The second electron is shaken-off due to the change in the correlation potential.

$$S_{SO} = \left[(2\pi)^3 iZ_p e^2/2\right]\iint \left[J_\mu^Z(p,p')\right]_r D(r-r_1) \left[J_\nu^\eta(p_1,b_1)\right]_\eta [\Phi(2,b_2,p_2)] d^4r d^4r_1 d^4r_2. \quad (1)$$

The projectile current at r with initial and final four-momenta p, p' respectively, is

$$\left(J_\mu^Z(p,p')\right)_r = M_p/(p_0 p_0')^{1/2}\, \bar{U}(p')\, \gamma_\mu U(p) \times \exp\{ir(p'-p)\} B_p^+ B_p. \quad (2)$$

The covariant electron current at r_1 with initial bound electron momentum b_1 and final free electron momentum p_1 is

$$\left(J_\nu^\eta(b_1,p_1)\right)_\eta = \left[m/(b_{10}p_{10})^{1/2}\right]\bar{u}(p_1)\gamma_\nu V(b_1,r_1) \times \psi(r_1,p_1)\, a_{p_1}^+ a_{b_1} \quad (3)$$

U and u are the Dirac spinors for projectile and free electron respectively. B's and a's are the annihilation operators for the projectile and the electron respectively. $V(b_1, r_1)$ is the bound electron spinor at r_1 with momentum b_1. If $\phi_{l_1}(l)$ be the Schrödinger solution for the bound electron, corresponding Dirac solution is given by [20]

$$V(b_1,r_1)\phi_{l_1}(l) = (1-\alpha\xi\gamma_0\gamma.\boldsymbol{n}/2)u(b_1)\phi_{l_1}(l) \times \exp(-ib_1.r_1), \quad (4)$$

where $\alpha = \dfrac{e^2}{\hbar c}$, ξ is the effective charge of the nucleus. $\gamma = (\gamma_0, \bar{\gamma})$ are the Dirac matrices, and $\bar{n}$ is the unit vector in the direction of $\bar{r}_1$. $\psi(r_1, p_1)$ in (3) is the wave function of the outgoing electron. In (1)

$$\Phi(2; p_2, b_2) = \bar{u}(p_2)V(b_2, r_2)\psi(2, p_2). \quad (5)$$

Shake-off electron from the second atom has initial and final four-momenta b_2 and p_2 respectively. For $i = 1, 2$ the four-momenta

$$b_i = (b_{i0}, \boldsymbol{b}_i).\ p_i = (p_{i0}, \boldsymbol{p}_i).\ p = (p_0, \boldsymbol{p}).\ p' = (p_0', \boldsymbol{p}')$$

with $b_{i0} = m - \varepsilon_i$, $p_{i0} = m + E_i$, $\boldsymbol{b}_i =$

and $p_0 = M_p + E$, $p_0' = M_p + E'$.

m is the electron mass and ε_i, E_i are the ionization energy and the kinetic energy of the ejected electrons.

$$pr = p_0 r_0 - \boldsymbol{p}.\boldsymbol{r}.$$

M_p is the projectile mass with kinetic energies E, E' before and after interaction respectively. The virtual photon

propagator $D(r-r_1)$ between the projectile and the interacting electron is equal to

$$D(r-r_1)=\int \frac{\exp(iq(r-r_1))}{(q^2+i\varepsilon)}d^4q. \tag{6}$$

The covariant interaction in the fourth order Feynman diagram (Figure 1b) which corresponds to the TS2 mechanism, is given by [21]

$$\begin{aligned} S_{TS2} &= (1/2)i^3e^4Z_p^2(2\pi)^3\int\left(J_\mu^c\ (p_1,b_1)\right)_{r_1}\\ &\times D(r-r_1)\left(J_\nu^c\ (p_2,b_2)\right)_{r_1} D(r_2-r')\\ &\times\left[\bar U(p')\exp(ir'p')\gamma_\mu S_I(r'-r)\exp(irp)\gamma_\nu U(p)\right]\\ &\times d^4r_1\,d^4r_2\,d^4r\,d^4r'. \end{aligned} \tag{7}$$

It contains two photon propagators $D(r_1-r)$ and $D(r_2-r')$ and a projectile propagator $S_I(r'-r)$.

$$S_I(r'-r)=\int\frac{\exp\{i(r'-r)S_p\}}{\hat S_p-M_p}d^4S_p,\quad \hat S_p=\gamma_\nu S_p^\nu; \tag{8}$$

$\left(J_\mu^c\ (p_1,b_1)\right)_{r_1}$ and $\left(J_\nu^c\ (p_2,b_2)\right)_{r_1}$ are the electron currents (3) at r_1 and r_2. The total matrix element for DI due to SO and TS2 mechanisms is

$$M_{fi}=(2\pi)^3\left\langle\psi_f\left|S_{SO}+S_{TS2}\right|\psi_i\right\rangle. \tag{9}$$

The initial state vector $|\psi_i\rangle$ and the final state vector $\langle\psi_f|$ for the interacting systems are respectively

$$\begin{aligned} \langle\psi_i| &= \psi_{H_i}(1,2)a_{b_1}^\dagger a_{b_2}^\dagger B_p^\dagger|0\rangle,\\ \langle\psi_f| &= a_{p_1}^\dagger a_{p_2}^\dagger B_{p'}^\dagger|0\rangle, \end{aligned} \tag{10}$$

$\psi_{H_i}(1,2)$ is the Weibaum type ground state correlated wave function of the hydrogen molecule [22].

$$\begin{aligned} \psi_{H_2}(1,2) &= N\left[\{\phi(r_{1a})\phi(r_{2b})+\phi(r_{2a})\phi(r_{1b})\}\right.\\ &\left.+\delta\{\phi(r_{1a})\phi(r_{2a})+\phi(r_{1b})\phi(r_{2b})\}\right]. \end{aligned} \tag{11}$$

Figure 2 gives the coordinates of the hydrogen molecule in a representative form.

$\delta=0.26$ and ϕ's are the ground state hydrogenic orbitals with effective charge $\xi=1.19$.

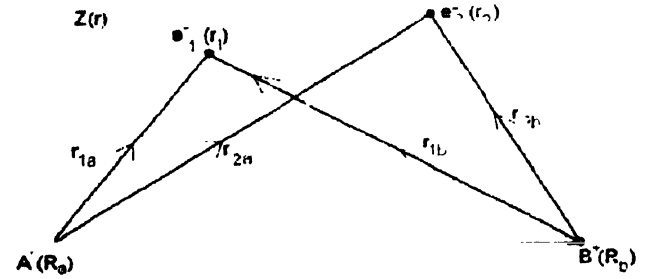

Figure 2. Representative diagram for space coordinates of H_2 and the projectile of charge Z. Polar coordinates with arbitrary origin are shown within the parenthesis. r_1 and r_2 are the coordinates of two bound electrons and R_a, R_b are the coordinates of two nuclei and r is that for the projectile.

The normalising constant [22] N is given by

$$N=1/[2(1+s)],$$

where $s=\left[1+\xi R_e+(\xi R_e)^2/3\right]\exp(-\xi R_e)$

R_e is the equilibrium separation between the two nuclei and

$$\begin{aligned} \phi(r_{1a}) &= C\exp(\xi r_{1a}),\\ C &= \xi^{3/2}/(\pi)^{1/2},\\ R_e &= 1.4\ \text{au}. \end{aligned}$$

2.1 Contribution from second order Feynman diagram (Figure 1a)

Let us first calculate the matrix element (9) for S_{SO}

$$S_2=(2\pi)^3\left\langle\psi_f\left|S_{SO}\right|\psi_i\right\rangle. \tag{12}$$

Substituting from (1) and integrating over r we obtain

$$S_2=(1/2)ie^2Z_p(2\pi)^4\int(2\pi)^4\delta^4(p_i-p_f)T_2I_2d^4q \tag{13}$$

The overlap integral I_2 is

$$\begin{aligned} I_2 &= (2\pi)^3\int\psi(r_1,p_1)\psi(2,p_2)\psi_{H_i}(1,2)\\ &\times\exp\{i(p-p')\cdot r_1\}d^3r_1\,d^3r_2\,d\tau, \end{aligned} \tag{14}$$

and $T_2=J_+J_1/(q_0^2-q^2)$,

$$\begin{aligned} J_+ &= U(p')\gamma_\mu U(p),\\ J_1 &= \bar u(p_1)\gamma_\nu u(b_1). \end{aligned} \tag{15}$$

Here, we use only the first term of the expansion in (4). The second term is neglected being small of the order of (1/137). The intergrals involved in I_2 are of the type

$$\begin{aligned} &\int\phi(r_{1a})\phi(r_{2b})\psi(r_1,p_1)\psi(2,p_2)\\ &\qquad\exp\{-ir_1\cdot(p-p')\}d^3\,1d^3\,2d\tau \end{aligned} \tag{16}$$

and $\int\phi(r_{1a})\phi(r_{2a})\psi(r_1,p_1)\psi(2,p_2)$

$$\times\exp\{-ir_1\cdot(p-p')\}d^3\,1d^3\,2d\tau,$$

$\psi(2,p_2)$ and $\psi(r_1,p_1)$ are the wave functions of the shake-off electron and the ionized electron respectively. The wave function $\psi(2,p_2)$ is either $\exp(-ir_{2b}\cdot p_2)$ or $\exp(-ir_{2a}\cdot p_2)$ depending on whether the corresponding integrals contain $\phi(r_{2b})$ or $\phi(r_{2a})$. From Figure 2, the coordinates of the ejected electrons are

$$\begin{aligned} r_1 &= r_{1a}+R_a=r_{1b}+R_b,\\ r_2 &= r_{2a}+R_a=r_{2b}+R_b. \end{aligned} \tag{16a}$$

Using (16a) for the first integral in (16)

$$\begin{aligned} &\int\phi(r_{1a})\phi(r_{2b})\exp(-ir_{2b}\cdot p_2)\exp\{-ir_1(p-p'-p_1)\}\\ &\qquad\cdot d^3\,1d^3\,2d\tau \end{aligned}$$

$$= C^2 \int \exp\{-\xi(r_{1a} - r_{2b})\} \exp(-ir_{1a} \cdot p_2)$$
$$\times \exp\{-i(r_{1a} + R_a).(p - p' - p_1)\} d^3 1 d^3 2 d\tau$$
$$= C^2 (2\pi)^3 \delta^3(p - p' - p_1)(8\pi\xi)^2 / [(\xi^2 + (p - p' - p_1)^2)^2 (\xi^2 + p^2)^2]. \quad (17)$$

We obtain similar expression for the second integral in (16). Noting the δ-function in (17) the overlap integral I_2 becomes

$$I_2 = N_{II_1} (2\pi)^6 2(1 + \delta)(8\pi\xi)^2 / [\xi^4 (\xi^2 + p_2^2)^2],$$
$$N_{II_1} = \xi/\pi . (1/2(1 + s)). \quad (18)$$

Integrating over q the matrix element for shake-off mechanism becomes

$$S_2 = i(2\pi)^3 (e^2/2) Z_p I_2 (2\pi)^4 \delta^4(p_i - p_f) J_2 J_1 \times [\eta^2 - (p - p')^2]^{-1}$$
$$= i(2\pi)^3 \frac{e^2}{2} (e^2/2) Z_p (2\pi)^4 \delta^4(p_1 - p_f) \times I_2 J_2 J_1 (\eta^2 - p_1^2)^{-1}. \quad (19)$$

$\eta = E_i^R - E_f^R$, P_i and P_f are the initial and final four-momenta of the interacting systems.

$$E_i^R = (p_0 + b_{10} + b_{20}),\ E_f^R = (p_0' + p_{10} + p_{20}),$$

Substituting

$$t_2 = (J_2 J_1)^* (J_2 J_1), \quad (20)$$

the DI amplitude from SO mechanism $S_2^* S_2$ becomes on using (19) and (20)

$$S_2 S_2^* = (2\pi)^6 \left(\frac{e^4}{4}\right) Z_p^2 [(2\pi)^4 \delta^4(P_i - P_f)]^2 \times I_2^2 t_2 (\eta^2 - p_1^2)^{-2}. \quad (21)$$

2.2. Two-step-two mechanism (TS2)

The matrix element for TS2 process is denoted by S_4 and

$$S_4 = (2\pi)^3 \langle \psi_f | S_{1S2} | \psi_i \rangle. \quad (22)$$

Using expressions (6) to (8), we obtain after some integrations

$$S_4 = -i(e^4/2)(2\pi)^3 Z_p^2 (2\pi)^4 \delta^4(p_i - p_f) I_4 J_1 J_2 J_2' \times [(p_1 - b_1)^2 (p_2 - b_2)^2 (S_2^2 - M_p^2)]^{-1}, \quad (23)$$

where $S_2 = (p - p_1 + b_1) = (p' + p_2 = b_2)$,

$$J_i = \bar{u}(p_i) \gamma_\mu u(b_i), \quad (24)$$
$$i = 1, 2,$$
$$J_2' = U(p') \gamma_\mu (S_2 + M_p) \gamma_\nu U(p)$$

and the overlap integral

$$I_4 = (2\pi)^3 \int \psi_{II_1}(1, 2) d^3 r_1 d^3 r_2 d\tau$$
$$= (2\pi)^6 N_{II_1} 2(1 + \delta)(8\pi\xi)^2 / (\xi^4)^2 \quad (24a)$$

The trace part of the γ-matrices (t_4) is

$$t_4 = (J_1 J_2 J_2')^* (J_1 J_2 J_2') = (J_1^* J_1)(J_2^* J_2)(J_2'^* J_2'). \quad (24b)$$

The amplitude for TS2 mechanism is obtained using (23) and (24) as

$$S_4^* S_4 = (e^8/4)(2\pi)^6 Z_p^4 [(2\pi)^4 \delta^4(p_i - p_f)]^2 \times I_4^2 t_4 (p_1 - b_1)^{-4} (p_2 - b_2)^{-4} (S_2^2 - M_p^2)^{-2}. \quad (25)$$

2.3. Interference of SO and TS2 terms :

Contribution to the DI amplitude due to interference of second order diagram (Figure 1a) and fourth order diagram (Figure 1b) is written as S_{2-4}.

From (19) and (23), we get

$$S_{2-4} = S_2^* S_4 + S_2 S_4^* = 2 S_2^* S_4$$
$$= -(2e^6/4)(2\pi)^6 Z_p^3 ((2\pi)^4 \delta^4(p_i - p_f))^2 I_2 I_4 \times [(\eta^2 - p_1^2)(p_1 - b_1)^2 (p_2 - b_2)^2 (S_2^2 - M_p^2)]^{-1} t_{24} \quad (26)$$

t_{24} represents the trace part in (26)

$$t_{24} = (J_Z J_1)^* (J_1 J_2 J_Z') = (J_Z^* J_Z')(J_1^* J_1) J_Z. \quad (27)$$

2.4. Cross section for double ionization :

The amplitude for double ionization is obtained using relations (21), (25) and (26)

$$|M_{fi}^2| = S_2^* S_2 + 2 S_2^* S_4 + S_4^* S_4$$
$$= 1/4 ((2\pi)^4 \delta^4(p_i - p_f))^2 I_4^2 (2\pi)^6 \times [Z_p^2 A(v) - 2 Z_p^3 B(v) + Z_p^4 C(v)], \quad (28)$$

where $A(v) = e^4 (I_2^2 / I_4^2)[t_2/(\eta^2 - p_1^2)^2]$, (29)

$$B(v) = e^6 (I_2 / I_4)[t_{24}/\{(\eta^2 - p_1^2)(p_1 - b_1)^2 (p_2 - b_2)^2 (S_2^2 - M_p^2)\}], \quad (30)$$

$$C(v) = e^8 [t_4/\{(p_1 - b_1)^4 (p_2 - b_2)^4 (S_2^2 - M_p^2)^2\}], \quad (31)$$

$\bar{v}$ = velocity of the projectile.

The cross section for double ionization becomes

$$\sigma^{2+} = \int [(2\pi)^4/4] \delta^4(p_i - p_f)(2\pi)^6 I_4^2 [1/|v|] \times |W_{fi}| \frac{d^3 p_1}{(2\pi)^3} \frac{d^3 p_2}{(2\pi)^3} \frac{d^3 p'}{(2\pi)^3}, \quad (32)$$

where $|W_{fi}| = Z_p^2 A(v) - Z_p^3 2 B(v) + Z_p^4 C(v)$. (33)

Let (θ_1, ϕ_2), (θ_2, ϕ_2) be the angles made by the two ionized electrons of momenta p_1 *and* p_2 respectively with the incident projectile momentum p. After integration over energy and momentum δ-functions and also over ϕ_1 and ϕ_2, we get

$$\sigma^{2+} = [(2\pi)^3/4] \int I_4^2 |W_{fi}| (1/|v|) |p_1| |p_2| dE_2 d\theta_1 d\theta_2. \quad (34)$$

Taking $E_2 = E_e$, the cross section for DI differential in E_e, θ_1 and θ_2 is

$$\frac{d^3\sigma^{2+}}{dE_e d\theta_1 d\theta_2} = [1/4](2\pi)^3 I_4^2 |W_{fi}|[1/|v|]|p_1||p_2|. \quad (35)$$

3. Results and discussion

Usually in high energy encounters (compared to the binding energy), the projectile moves forward with little loss of energy and momentum [20]. Under the situation, the ejected electrons will carry the binding energy released during double ionization. We compute the differential cross section for equal sharing of the binding energy by the electrons ejected forward.

With these assumptions, we calculate $A(v)$, $B(v)$ and $C(v)$ in (33). Knowing that $E, E' << M_p$ and $E_1 - E_2 = E_e = \varepsilon = 15.6$ eV (average ionization energy of the electrons) we can write for low momentum transfer of the projectile

$$pp' \approx M_p^2$$

and $$p_1 b_1 = p_2 b_2 \approx m^2 \quad (36)$$

and obtain from (15), using usual γ-matrix relations [21]

$$\begin{aligned} t_2 &= (J_2^* J_2)(J_1^* J_1) \\ &= 1/(4m^2 M_p^2)\left[\{p_\mu p'_\nu + p_\nu p'_\mu - g_{\mu\nu}(pp' - M_p^2)\}\right. \\ &\quad \left.\times \{p_{1\mu} b_{1\nu} + p_{1\nu} v_{1\mu} - g_{\mu\nu}(p_1 b_1 - m^2)\}\right] \\ &= \left|1 + \frac{E + E'}{2M_p}\right| \end{aligned} \quad (37)$$

From (24), we obtain after lengthy computation

$$\begin{aligned} t_4 &= (J_1 J_2 J_2')^*(J_1 J_2 J_2') = (J_1^* J_1)(J_2^* J_2)(J_2'^* J_2') \\ &\approx 4M_p^2. \end{aligned} \quad (38)$$

From eq. (27),

$$t_{24} = (J_2 J_2'^*)(J_1 J_1^*) J_2^*$$

where $$\begin{aligned} (J_2 J_2'^*) &= \left(\bar{U}(p')\gamma_\mu U(p)\right)\left(\bar{U}(p)\gamma_\mu(\hat{S}_2 + M_p)\right. \\ &\quad \left.\times \gamma_\mu U(p')\right) \\ &= 1/2(1/4M_p^2) Tr\left[(\hat{p}' + M_p)\gamma_\mu(\hat{p} + M_p)\gamma_\nu\right. \\ &\quad \left.\times (\hat{S}_2 + M_p)\gamma_\mu\right]. \end{aligned} \quad (39)$$

To write J_2, we use Gordon decomposition [21], and obtain

$$\begin{aligned} J_2^\mu &= \bar{u}(p_2)\gamma_\mu u(b_2) = \bar{u}(p_2)\left(\frac{p_2 + b_2}{2m}\right. \\ &\quad \left.\times u(b_2) + \bar{u}(p_2)\sigma_{\mu\nu}(p_2 - b_2)^\nu u(b_2)\right). \end{aligned} \quad (40)$$

Since mass is much larger than kinetic energy in the case of p_2 and $b_2[=(b_{20}, o)]$, we can assume

$$J_2^\mu = \left(\frac{p_2 + b_2}{2m}\right)^\mu \quad (41)$$

and since

$$J_1 J_1^* = \frac{1}{2m^2}\left[p_{1\mu} b_{1\nu} + p_{1\nu} b_{1\mu} - g_{\mu\nu}(p_1 b_1 - m^2)\right], \quad (42)$$

we get after some computation

$$t_4 \approx M_p \quad (43)$$

Accordingly, we can approximate the factors in the denominators of $A(v)$, $B(v)$ and $C(v)$ as below.

$$\begin{aligned} &(\eta^2 - p_1^2) = 4\varepsilon^2 - 2m\varepsilon \approx -2m\varepsilon, \\ &(p_1 - b_1)^2 = (p_1 - b_1)^2 = -2m(E_e - \varepsilon) + 2E_e\varepsilon = 2\varepsilon^2, \\ &\because E_e = \varepsilon, \\ &M_p^2 \approx 4M_p\varepsilon\left|1 + \frac{\varepsilon}{M_p}\right. \end{aligned} \quad (44)$$

Substituting from (37), (38), (43) and (44), we get

$$\begin{aligned} A(v) &= e^4(I_2^2/I_1^2)\left(1 + \frac{E + E'}{2M_p}\right)/(-2m\varepsilon)^2, \\ 2B(v) &= e^6(I_2/I_1)\left[2M_p/\left[(-2m\varepsilon)(2\varepsilon^2)\right]^2\right. \\ &\quad 4M_p\varepsilon\left|1 + \frac{\varepsilon}{M_p}\right. \\ C(v) &= e^8 4M_p^2/(2\varepsilon^2)^2 16M_p^2\varepsilon^2\left|1 + \frac{\varepsilon}{M_p}\right. \end{aligned} \quad (45)$$

From (45), we find that $B(v)$ is positive. For equivelocity projectiles, ratio R of the cross sections induced by negative projectiles (Z_-) to that induced by positive projectiles (Z_+) is given by

$$R \quad \begin{matrix} Z_-^2 A(v) - Z_-^3 2B(v) + Z_-^4 C(v) \\ Z_+^2 A(v) \quad Z_+^3 2B(v) + Z_+^4 C(v) \end{matrix} \quad (46)$$

Since $B(v)$ is +ve, the DI cross section induced by electron is greater than that induced by proton. For $E, E' << M_p$, we find $A(v)$, $B(v)$ and $C(v)$ are weakly dependent on E. Hence, R is almost constant in the energy range under consideration. Atomic units are used throughout the calculation.

We have computed the cross sections for double ionization of H_2 by equivelocity projectiles e^-, p^+, $_3He^{2+}$ and $_7Li^{3+}$ in the energy range 0.75 MeV/amu to 3.5 MeV/amu for projectile emission in the forward direction. The result is compared with the experimental result of the Georgia Group [14a,b] in Figures (3–5) and in Table 1. Ratios of the cross sections of the projectile ions relative to proton are shown in Table 2. For e^- and p^+ projectiles, the present results (Figures 3,4) agree well with the experiments. But the present result for $_3He^{2+}$ projectile is much below the latest experimental result. In the case of He^{2+}, the projectile beam contains a mixture of $_3He^{2+}$ and $_4He^{2+}$ isotopes, whereas theoretically, we can take only odd-half-spin $_3He^{2+}$ projectile in the Feynman diagram. This may be one of the reasons for large difference between theoretical and experimental results in $_3He^{2+}$. With $_7Li^{3+}$ projectile there is no experiment as yet.

With the projectile energy range under consideration, the projectile-bound electron interaction time is much smaller than the nuclear rotation and vibration time. As such, one may assume that the double ionization and subsequent fragmentation may occur from the ground state of the molecule. It is also obvious that the cross section depends on the choice of the wave function of the H_2 molecule and the different correlation parameters. Better wave function along with inclusion of Coulomb distortion in the emitted electron wave function, will certainly show some improvement on our result.

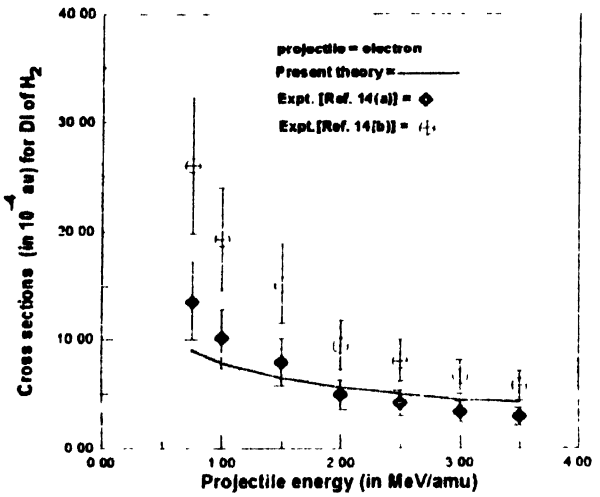

Figure 3. Cross section for double ionization of H_2 by electron as projectile *versus* kinetic energy of the projectile

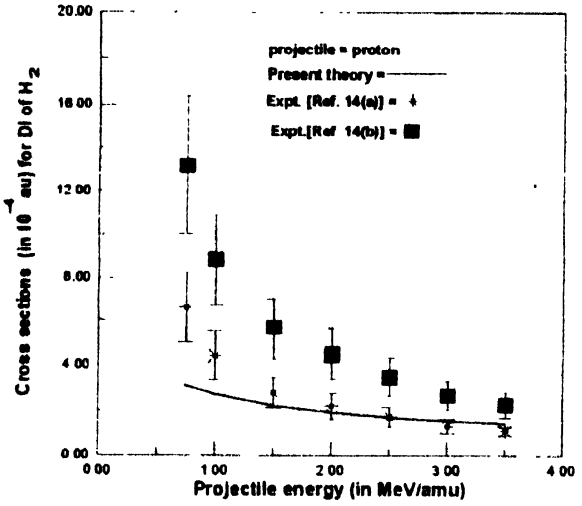

Figure 4. Same as in Figure 3 by proton

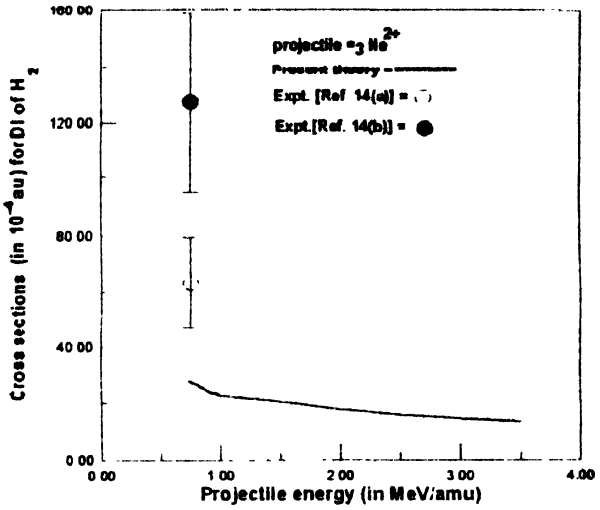

Figure 5. Same as in Figure 3 by $_3He^{2+}$

From (33), we find that the cross section depends on the sign of the projectile charge Z_p through coefficient of the interference term Z_p^3. This shows essentially, the double ionization phenomena is a combined effect of first-Born and second-Born interactions. Further, we find that $B(v)$ in (45) is positive. As long as $B(v)$ is positive, DI induced by electron is greater than that induced by proton. The average ratio of the DI cross sections induced by electron to that induced by proton is 2.8 in the present case, while the experimental value for the ratio by the Georgia group is 2.4. To reduce the gap between the experimental and the theoretical values, one should take more accurate wave functions in the

Table 1. Cross sections for double ionisation of H_2 by e⁻, p^+, $_3He^{2+}$ and $_3Li^{3+}$ with the emission of electrons, each of energy 15.6 eV, in the forward direction of the projectiles. FT is the present field theoretic result. Experimental results are from Refs [14a,b]

Projectile energy (MeV/amu)	Cross sections (in 10^{-4} au) for double ionisation of H_2									
	e			p^+			$_3He^{2+}$			$_3Li^{3+}$
	Expt			Expt			Expt			
	FT	(a)	(b)	FT	(a)	(b)	FT	(a)	(b)	FT
0.75	9 076	13.6 ± 2	26 1 ± 3 9	3 155	6 6 ± 1	13 2 ± 2	28 34	63 5 ± 10	127 ± 20	140 105
1 0	7 875	10 1 ± 1 5	19 3 ± 2.9	2 73	4.41 ± 0 65	8 82 ± 1.32	22 504	–	–	121.32
1.5	6 42	7.92 ± 1.2	15 2 ± 2 3	2 23	2 81 ± 0 42	5 63 ± 0.84	20.2	–	–	99.012
2 0	5 567	4.94 ± 0 73	9 49 ± 1 42	1 93	2 22 ± 0.34	4.49 ± 0.67	17.325	–	–	85.7
2.5	4 98	4 2 ± 0 63	8 06 ± 1 21	1 73	1.75 ± 0 26	3 497 ± 0 52	155	–	–	76.7
3.0	4 545	3.43 ± 0 52	6 58 ± 0.99	1 58	1.35 ± 0 2	2.69 ± 0.4	14 15	–	–	70.04
3.5	4.20	3.01 ± 0 45	5 77 ± 0 87	1 46	1.14 ± 0 12	2 28 ± 0 34	13 1	–	–	64.825

overlap integrals I_2 and I_4. With the present limitation, our result for the ratio agrees fairly well with that of the experiment, for the projectile pair (e ,p). In the case of ($_3He^{2+}$,p$^+$) pair, the present ratio is 8.99, which is almost equal to Z_p^3. Corresponding experimental value is 9.6 For ($_7Li^{3+}$,p$^+$) pair, the present ratio is 44.4 This result, though greater than Z_p^3, is much less than Z_p^4. Departure from Z_p^3 behaviour in the case of ($_7Li^{3+}$,p$^+$) pair may be attributed to the dominance of the double collision process over shake-off mechanism as Z-value of the projectile increases

Table 2. Ratios of the cross sections for DI by different projectiles to that by proton FT is the present field theoretic results Experimental results are from Table 1

Projectile energy (MeV/amu	Cross sections (in 10^{-4} au) for double ionisation of H_2						
	e /p			$_3He^{2+}$/p			Li^{3+}/p
	FT	Expt (a)	Expt (b)	FT	Expt (a)	Expt (b)	FT
0 75	2 88	2 06	1 98	8 98	9 62	9 62	44 4
1 0	2 88	2 29	2 19	8 24			41 43
1 5	2 88	2 82	2 7	9 05			11 4
2 0	2 88	2 23	2 11	8 97			11 4
2 5	2 88	2 4	2 3	8 96			44 34
3 0	2 88	2 54	2 45	8 96			14 33
3 5	2.88	2 64	2 53	8 97			44 4

For all the projectiles, we find from (44) that for $k_e \neq \varepsilon$, the square of the differences in 4-momenta of the emitted electrons become

$$(p_1 - k_1)^2 - (p_2 - k_2)^2 = -2m(E_e - \varepsilon) + 2k_e\varepsilon \approx -2m(I_e - \varepsilon)$$

Hence, $B(v)$ and $C(v)$ in eq. (45) become small of the order of 10^{-12} and 10^{-21} respectively compared to $A(v)$. Eventually, the TS2 mechanism will have negligible contribution on the double ionisation of H_2. So, one can conjecture that for emitted electron-energy not equal to the ionisation energy ε, the double ionisation becomes almost independent of sign of the charge. An experimental verification of the conjecture is expected.

4. Conclusion

Through the present paper we have proved in a field theoretic way that the double ionisation by negative projectile is greater than that by a positive one. In the case of $_3He^{2+}$ and $_7Li^{3+}$ projectiles as argued in our earlier paper [15], we have assumed these bare ions as odd spin-1/2 particles. The projectile energies though small compared to their rest mass, are much higher than the binding energies of the ionised electrons. So, one may assume the electrons in the molecule to behave as free particles in presence of the high energy projectiles. Eventually, there is no loss of generality to represent the electrons with Feynman directed lines History of these electrons being localised in the molecule appears through the wave functions contained in the overlap integrals As such, the correlation term through the proper choice of wave function, plays an important role in the double ionisation process

We like to emphasize that application of gauge invariant language of QED in ion-atom collision phenomena, though rare, is most general. In the low energy limit, QED exhibits classical behavior But because of the fully covariant treatment from the onset, one may expect to get different result in QED technique as compared to the result obtained by extending classical result to the covariant relativistic limit The expressions T_2, T_{34} and T_1 (eqs 15,27,24b) containing covariant currents and propagators, give rise to the QED effect

Finally, the present field theoretic result for the ratio of the double ionisation cross section by (e ,p$^+$) pair agrees fairly well with that of the experiment In the case of ($_3He^{2+}$,p$^+$) pair, the Z_p^3 dependence of the ratio highlights the importance of the interference between the second order and fourth order S-matrix However, with the increase of the Z-value, the fourth order S-matrix dominates over that of the second order, showing deviation from Z^3 law.

Acknowledgment

The author (S B.) wishes to thank A K Edwards for supplying the latest experimental data obtained by the Georgia Group prior to publication. This research was supported by the University Grants Commission, New Delhi, under grant No F-10-17/98 (SR-I).

References

[1] J Krishnakumar B Bapat J A Rajgara and M Krishnamurthy *J Phys* **B27** L777 (1994)

[2] B Bapat J Krishnakumar C P Safvan M J Singh R Shankar and S K Goel *Phys Rev* **A54** 2925 (1996)

[3] J Krishnakumar and S K Srivastava *J Phys* **B27** L251 (1994)

[4] R M Wood A K Edwards and R J Fitzell *Phys Rev* **A34** 4415 (1986)

[5] M B Shah and H B Gilbody *J Phys* **B18** 899 (1985)

[6] M Charlton J H Anderson J Brun-Nielsen B J Deutch P Hvelplund J M Jacobsen H Knudsen G Laricchia M R Poulsen and J O Pedersen *J Phys* **B21** L545 (1988)

[7] R D Dubois and L H Toburen *Phys Rev* **A38** 3690 (1988)

[8] J Y Kamber C J Cocke S Cheng and S L Varghese *Phys Rev Lett* **60** 2026 (1988)

[9] J F Reading and A L Ford *J Phys* **B21** L685 (1988), **B20** 3747 (1987)

[10] J H McGuire *Phys Rev Lett* **49** 1153 (1982) **A36** 1114 (1987)

[11] J Watanabe and J Vegh *Nucl Instrum Meth* **B40/41** 89 (1989)

[12] J F Reading and A L Ford *Phys Rev Lett* **58** 543 (1987)

[13] A K Edwards R M Woods A S Beard and R J Fitzell *Phys Rev* **A37** 3697 (1988)

[14] (a) A K Edwards, R M Woods, J L Davis and R L Ezell *Phys Rev.* **A42** 1367 (1990), (b) A K Edwards, R M Woods and R L Ezell *Phys Rev* **A42** 1799 (1990)

[15] S Bhattacharyya, K Rinn, E Salzborn and L Chatterjee *J Phys* **B21** 111 (1988)

[16] S Bhattacharyya *Phys Scri* **42** 159 (1990)

[17] S Bhattacharyya and K Pathak *Phys Scri* **54** 143 (1996)

[18] L Haris and C M Brown *Phys Rev* **105** 1656 (1957)

[19] S Bhattacharyya and S Mitra *Phys Rev.* **A60** 2269 (1999)

[20] A I Akhiezer and V B Berestetsky *Quantum Electrodynamics* (New York . Interscience) (1965)

[21] J D Bjorken and S D Drell *Relativistic Quantum Mechanics* (New York · McGraw-Hill) (1964)

[22] P Gupta and S P Khare *J Chem Phys* **68** 2193 (1978)